Interactions between calmodulin and neurogranin govern the dynamics of CaMKII as a leaky integrator

Mariam Ordyan[1,2], Tom Bartol[2], Mary Kennedy[3], Padmini Rangamani[4*], and Terrence Sejnowski[1,2*]

[1]Institute for Neural Computation, University of California San Diego

[2]Computational Neurobiology Laboratory, Salk Institute for Biological Sciences

[3]The Division of Biology and Biological Engineering, California Institute of Technology

[4]Department of Mechanical and Aerospace Engineering, University of California, San Diego

[*]Corresponding authors: Padmini Rangamani, prangamani@ucsd.edu, Terrence Sejnowski, terry@salk.edu

October 17, 2019

Abstract

Calmodulin-dependent kinase II (CaMKII) has long been known to play an important role in learning and memory as well as long term potentiation (LTP). More recently it has been suggested that it might be involved in the time averaging of synaptic signals, which can then lead to the high precision of the information stored at a single synapse. However, the role of the scaffolding molecule, neurogranin (Ng), in governing the dynamics of CaMKII are not yet fully understood. In this work, we adopt a rule-based modeling approach through the Monte Carlo method to study the effect of Ca^{2+} signals on the dynamics of CaMKII phosphorylation in the postsynaptic densities (PSD). Calcium surges are observed in the synaptic spines during an EPSP and back-propagating action potential due to the opening of NMDA receptors and voltage dependent calcium channels. We study the differences between the dynamics of phosphorylation of CaMKII monomers and dodecameric holoenzymes. The scaffolding molecule Ng, when present in significant concentration, limits the availability of free calmodulin (CaM), the protein which activates CaMKII in the presence of calcium. We show that it plays an important modulatory role in CaMKII phosphorylation following a surge of high calcium concentration. We find a non-intuitive dependence of this effect on CaM concentration that results from the different affinities of CaM for CaMKII depending on the number of calcium ions bound to the former. It has been shown previously that in the absence

of phosphatase CaMKII monomers integrate over Ca^{2+} signals of certain frequencies through autophosphorylation (Pepke et al, Plos Comp. Bio., 2010). We also study the effect of multiple calcium spikes on CaMKII holoenzyme autophosphorylation, and show that in the presence of phosphatase CaMKII behaves as a leaky integrator of calcium signals, a result that has been recently observed *in vivo*. Our models predict that the parameters of this leaky integrator are finely tuned through the interactions of Ng, CaM, CaMKII, and PP1. This is a possible mechanism to precisely control the sensitivity of synapses to calcium signals.

1 Introduction

Information is stored in the brain through synaptic plasticity. It has been reported that synaptic strength is highly correlated with the size of the spine head, and the precision of information stored at a single synapse is much higher than one might have expected, given the stochastic variability of synaptic activation [4, 48, 44]. Structural changes to the postsynaptic spine that can lead to spine enlargement and thus structural plasticity are triggered by Ca^{2+} signaling [30, 47]. Time averaging of these calcium signals has been suggested as a plausible mechanism for achieving the high precision of information processing observed in spines. Furthermore, phosphorylation of calcium/calmodulin-dependent protein kinase II (CaMKII) has been postulated as the most probable pathway satisfying the long time scales predicted for averaging [4].

CaMKII is an autophosphorylating kinase; in postsynaptic densities (PSD), CaMKII has been shown to play an important role in learning and memory [38]. Specifically, mice with a mutation in a subtype of CaMKII exhibit deficiencies in long-term potentiation (LTP) and spatial learning [62, 63]. Moreover, CaMKII expression regulates the rate of dendritic arborization and the branch dynamics [75, 69]. This indicates its importance for structural plasticity. Since CaMKII has been shown to bind actin, the major cytoskeletal protein in dendritic spines this is not [9, 49] this is not surprising.

Activation of CaMKII is exquisitely regulated by multiple steps. As the name suggests, CaMKII is activated by calmodulin (CaM) [6], which is a protein with 4 Ca^{2+} binding sites: 2 on its C-terminal and 2 on N-terminal (Figure 1a) [70, 21]. It binds Ca^{2+} cooperatively and is able to activate CaMKII more potently if it has more Ca^{2+} ions bound to it [61]. In the absence of Ca^{2+}, CaM is bound to scaffolding protein neurogrnanin (Ng,) which dramatically reduces its affinity for Ca^{2+} (Figure 1b). On the other hand, Ca^{2+} decreases CaMs binding affinity for Ng [31]. Thus, CaM activation and therefore CaMKII activation depend on the competitive effects of Ca^{2+} and Ng.

Further complexity for CaMKII activation is built into the structure of the molecule itself. CaMKII is a dodecamer arranged in 2 stacked hexomeric rings [6, 15]. The monomers of CaMKII (mCaMKII) consist of the kinase domain, CaM-binding domain, and phosphorylation sites T286(287), and T305(306) [58, 27, 39, 28, 51]. When the CaM-binding domain is unoccupied, and the T286(287) site is unphosphorylated, the monomer is in a conformation such that the kinase is inactive (Figure 1c, top). When CaM is bound to CaMKII monomer, the latter undergoes a con-

formational change, such that the kinase is now active. Active CaMKII can phosphorylate other Ca^{2+}/CaM-bound CaMKII monomers (a process known as CaMKII autophosphorylation). A CaMKII monomer can only be phosphorylated if the calmodulin bound to it has at least one calcium ion, and once phosphorylated it remains in the active state even after unbinding from CaM (Figure 1c middle). In this manner, Ca^{2+} influx initiates a prolonged CaMKII activation that can long outlast the brief calcium stimulus [42, 43, 26, 32, 39]. Various types of protein phosphatases (PP1, PP2A, PP2B, PP2C) can dephosphorylate CaMKII in the brain and, if CaM is not bound to the latter, bring it back to its inactive state [51, 16]. In the post-synaptic density (PSD) however, mainly protein phosphatase 1 (PP1) has been shown to be responsible for CaMKII dephosphorylation [16, 65] (Figure 1c bottom). Within the holoenzyme each of the monomers can phosphorylate neighbors, as long as the former is active and the latter has CaM bound to it (Figure 1d) [27, 57]. The phosphorylation rate depends on how many Ca^{2+} ions are bound to the CaM bound to the substrate [53].

Here we sought to examine how the competition between Ca^{2+}-mediated CaM activation and Ng scaffolding of CaM affects the response of CaMKII to calcium signals. To do so, we developed a computational model that accounts for both CaMKII monomeric activation and the holoenzyme kinetics in an agent-based framework. This model is built on a previously published model of CaMKII monomers activation by Ca^{2+}/CaM [53] and includes the role of the scaffolding molecule Ng and the protein phosphatase PP1. Finally we build a model of a dodecameric holoenzyme, and study the effects of multiple Ca^{2+} spikes on CaM-CaMKII-PP1 system in the presence and absence of Ng. Using this model we investigated the dynamics of CaMKII phosphorylation as a function fo Ca^{2+}-influx dynamics and interactions with Ng. Results from our model show that CaMKII behaves as a leaky integrator, as proposed in experiments and more importantly, Ng tunes the behavior of the leaky integrator.

2 Methods

We developed the following models to characterize CaMKII phosphorylation at increasing levels of complexity. First we added the scaffolding molecule Ng to the model from *Pepke et al* [53], to investigate its effect on CaMKII phosphorylation dynamics. Second, we added PP1 to this model to simulate the phosphorylation-dephosphorylation cycle and characterize the effects of Ng on this system. Finally, we built a model of a dodecameric holoenzyme and looked at the response of the holoenzyme-phosphatase system to calcium signals and how it is affected by Ng.

2.1 Model description

2.1.1 Model of CaMKII monomers

We begin with the model of CaMKII monomers (mCaMKII) described by Pepke et al. [53]. This model includes Ca^{2+} binding rates to CaM, CaM binding rates to mCaMKII, and phosphorylation rates of active CaMKII monomers by one another, all depending how many Ca^{2+} ions are bound to

the CaM molecules involved. We incorporate Ng binding to CaM with the rate constants from [56], and assume that Ca^{2+} and Ng bind CaM mutually exclusively (Table1). Since the Pepke model was designed to study processes on a short time-scale and did not include dephosphorylation, the final product of that model is the phosphorylated CaMKII, which is bound to CaM. In reality, however, although CaMKII phosphorylation is known to "trap" CaM, the latter can still unbind from (and bind to) phosphorylated CaMKII, albeit with slower kinetics [41]. For the timescales we are interested in this is an important reaction, and we adapt these reaction rates from [41]. Finally CaMKII dephosphorylation is modeled as Michaelis-Menten kinetics, with the rate constants from [11] (Table 1).

2.1.2 CaMKII holoenzyme model

To model the dynamics of CaMKII holoenzyme we changed the types of molecules that we start the simulation with. Instead of CaMKII monomers, we initiated the simulation with CaMKII holoenzymes, and defined the phosphorylation rules for individual subunits interactions such that a given subunit can only phosphorylate one of its neighbors (see model assumptions). The rules are the same as those of the monomers, with the exception of 2 CaMKII monomers binding each other to phosphorylate one another, since they are already bound within the holoenzyme. Except now they refer to CaMKII subunits within the holoenzyme rather than CaMKII monomers.

This model does not contain any CaMKII monomers outside of the holoenzyme. We calculated the total number of the holoenzymes to keep the concentration of the $[mCaMKII] = 80$ µM consistent with our model of the monomers. For our simulated PSD volume $V = 0.0156$ µm^3 this concentration corresponds to 80 µM $= 80 \cdot (6.022 \cdot 10^{23} \cdot 0.0156 \cdot 10^{-15}) \cdot 10^{-6}$ monomers which constitutes $752/12 \approx 63$ holoenzymes.

2.1.3 Model assumptions

An important caveat of this model is that only one of the phosphorylation sites (T286/7) is incorporated here. The phosphorylation of T305/6 site is a slower reaction that is known to inhibit CaM binding to T286/7-unphosphorylated CaMKII subunit [18], and is omitted from our simulations.

It has been shown that while the kinase domains of individual subunits are attached to the rigid hub domain with highly flexible linker domain, $\sim 20\%$ of subunits form dimers, and $\sim 3\%$ of them are in a compact conformation both of which render CaM-binding-domain inaccessible [45]. The model presented in this work does not include such detailed interactions between and flexibility of the individual subunits within the holoenzyme. Rather we assume that the kinase domains are positioned rigidly within the 2 hexomeric rings, such that each subunit is in position to phosphorylate only one of its neighbors as depicted on Figure 1d.

We further assume that the CaMKII subunits within the holoenzyme have the same binding rates to different species of Ca^{2+}/CaM as the CaMKII monomers, and once activated their phosphorylation rate is the same as that of the corresponding monomers.

Based on these assumptions the model for the holoenzyme lacks the reaction for 2 CaMKII

monomers binding to phosphorylate one another. Rather, once the appropriate neighbor of an active CaMKII subunit binds Ca^{2+}/CaM the phosphorylation rule is invoked with the corresponding reaction rate (Table 1).

2.2 Rule-Based modeling and BioNetGen

Since each CaMKII monomer can bind a calmodulin molecule, which can adopt 9 distinct states (assuming that the 2 Ca^{2+} binding sites on each of the lobes are indistinguishable), and be phosphorylated or unphosphorylated, there are more than 18^{12} states the dodecameric holoenzyme could adopt. To avoid a combinatorial explosion we built our model in a rule-based modeling language BioNetGen [29], which is briefly describe here.

A powerful idea in the heart of rule-based modeling is colloquially referred as "don't care don't write" [20, 8]. Here, for a given reaction (rule), we only specify the states of the reactants that are relevant for the said reaction, and leave the rest unspecified. For example a given CaMKII subunit will bind a given species of Ca^{2+}/CaM with the same rate regardless of the conformation of its neighbors. Thus a rule to bind a CaM molecule that has 2 Ca^{2+} ions bound to its C lobe would look like:

$$\text{CaMKII}(286\sim U, cam) + CaM(camkii, C \sim 2, N \sim 0) <->$$
$$\text{CaMKII}(286\sim U, cam!1).CaM(camkii!1, C \sim 2, N \sim 0), \quad k_{on}^{CaM2C},\ k_{off}^{CaM2C}$$

This rule indicates that regardless of the presence or conformations of a non-phosphorylated (indicated by $286 \sim U$) CaMKII subunits' neighbors it binds CaM, with 2 Ca^{2+} ions at its C lobe, reversibly with the reaction rates k_{on}^{CaM2C} and k_{off}^{CaM2C} (Table 1). This dramatically reduces the number of reactions that need to be written. In the case of CaMKII model, we only end up with ~ 40 reactions despite the huge number of possible states.

In BioNetGen, once the reactions have been specified, if there is no danger of running into combinatorial explosion (the numbers of possible states and reactions are manageable), a full network of reactions can be generated, and the simulations can be run with ODEs. If the number of states of a given enzyme is too large however, a stochastic agent-based approach is adopted, in which case only the reactions between existing discrete molecules that occur during the simulation need to be tracked by the program (network free simulation [64, 67]). In this case the important quantity is the number of different states present which can be much smaller than the number of possible states.

In our case, we run the simulations for our monomer model with ODEs, and network free for the holoenzyme model.

Parameter	Value	Reference
Ca^2 binding to CaM		
k_{on}^{1C}	4 $\mu M^{-1}s^{-1}$	[53, 37, 34, 61]
k_{off}^{1C}	40.24s^{-1}	[54, 40, 25]
k_{on}^{2C}	10 $\mu M^{-1}s^{-1}$	[53, 37, 34, 61]
k_{off}^{2C}	9.3 s^{-1}	[25]
k_{on}^{1N}	100 $\mu M^{-1}s^{-1}$	[53, 37, 34, 61]
k_{off}^{1N}	2660 s^{-1}	[54, 25, 52, 12]
k_{on}^{2N}	150 $\mu M^{-1}s^{-1}$	[53, 37, 34, 61]
k_{off}^{2N}	990 s^{-1}	[54, 40, 25, 52, 12]
CaM binding to unphosphorylated CaMKII		
k_{on}^{CaM0}	$3.8 \cdot 10^{-3}$ $\mu M^{-1}s^{-1}$	[53, 41]
k_{off}^{CaM0}	6.56 s^{-1}	[53, 41]
k_{on}^{CaM1C}	$59 \cdot 10^{-3}$ $\mu M^{-1}s^{-1}$	[53, 41]
k_{off}^{CaM1C}	6.72 s^{-1}	[53, 41]
k_{on}^{CaM2C}	0.92 $\mu M^{-1}s^{-1}$	[53, 41]
k_{off}^{CaM2C}	6.35 s^{-1}	[53, 41]
$k_{on}^{CaM1C1N}$	0.33 $\mu M^{-1}s^{-1}$	[53, 41]
$k_{off}^{CaM1C1N}$	5.68 s^{-1}	[53, 41]
$k_{on}^{CaM2C1N}$	5.2 $\mu M^{-1}s^{-1}$	[53, 41]
$k_{off}^{CaM2C1N}$	5.25 s^{-1}	[53, 41]
k_{on}^{CaM1N}	$22 \cdot 10^{-3}$ $\mu M^{-1}s^{-1}$	[53, 41]
k_{off}^{CaM1N}	5.75 s^{-1}	[53, 41]
k_{on}^{CaM2N}	0.1 $\mu M^{-1}s^{-1}$	[53, 41]
k_{off}^{CaM2N}	1.68 s^{-1}	[53, 41]
$k_{on}^{CaM1C2N}$	1.9 $\mu M^{-1}s^{-1}$	[53, 41]
$k_{off}^{CaM1C2N}$	2.09 s^{-1}	[53]
k_{on}^{CaM4}	30 $\mu M^{-1}s^{-1}$	[53, 41]
k_{off}^{CaM4}	1.95 s^{-1}	[53, 41]
Ca^2 binding to CaM-CaMKII		
k_{on}^{K1C}	44 $\mu M^{-1}s^{-1}$	[53, 25]
k_{off}^{K1C}	29.04 s^{-1}	[53, 25]
k_{on}^{K2C}	44 $\mu M^{-1}s^{-1}$	[53, 25]
k_{off}^{K2C}	2.42 s^{-1}	[53, 25]
k_{on}^{K1N}	75 $\mu M^{-1}s^{-1}$	[53, 25]
k_{off}^{K1N}	301.5 s^{-1}	[53, 25]
k_{on}^{K2N}	76 $\mu M^{-1}s^{-1}$	[53, 25]
k_{off}^{K2N}	32.68 s^{-1}	[53, 25]

Parameter	Value	Reference
CaMKII binding to CaM-CaMKII $*$		
k_{on}^{CaMKII}	50 $\mu M^{-1}s^{-1}$	[53, 17]
k_{off}^{CaMKII}	60 s^{-1}	[53, 27, 10]
CaMKII phosphorylation		
k_p^{CaM0}	0 s^{-1}	[53, 61]
k_p^{CaM1C}	0.032 s^{-1}	[53, 61]
k_p^{CaM2C}	0.064 s^{-1}	[53, 61]
$k_p^{CaM1C1N}$	0.094 s^{-1}	[53, 61]
$k_p^{CaM2C1N}$	0.124 s^{-1}	[53, 61]
k_p^{CaM1N}	0.061 s−1	[53, 61]
k_p^{CaM2N}	0.12 s^{-1}	[53, 61]
$k_p^{CaM1C2N}$	0.154 s^{-1}	[53, 61]
k_p^{CaM4}	0.96 s^{-1}	[53, 61]
CaM binding to phosphorylated CaMKII		
$k_{p,on}^{CaM0}$	$1.27 \cdot 10^{-3}$ $\mu M^{-1}s^{-1}$	[53, 41]
$k_{p,on}^{CaM1C}$	19.7 $\mu M^{-1}s^{-1}$	[53, 41]
$k_{p,on}^{CaM2C}$	0.3 $\mu M^{-1}s^{-1}$	[53, 41]
$k_{p,on}^{CaM1C1N}$	1.1 $\mu M^{-1}s^{-1}$	[53, 41]
$k_{p,on}^{CaM2C1N}$	1.73 $\mu M^{-1}s^{-1}$	[53, 41]
$k_{p,on}^{CaM1N}$	7.3 $\mu M^{-1}s^{-1}$	[53, 41]
$k_{p,on}^{CaM2N}$	0.03 $\mu M^{-1}s^{-1}$	[53, 41]
$k_{p,on}^{CaM1C2N}$	0.63 $\mu M^{-1}s^{-1}$	[53, 41]
$k_{p,on}^{CaM4}$	10 $\mu M^{-1}s^{-1}$	[53, 41]
$k_{p,off}^{CaM}$	0.07 s^{-1}	[41]
Ng binding to CaM		
k_{on}^{Ng}	5 $\mu M^{-1}s^{-1}$	[56]
k_{off}^{Ng}	1 s^{-1}	[56]
CaMKII dephosphorylation by PP1 (Michaelis-Menten constants)		
k_{cat}	0.41 s^{-1}	[11]
K_m	11 μM	[11]

Table 1: Reaction rates for our model. $*$ only present in the model for monomers

3 Results

3.1 mCaMKII phosphorylation dose response curve depends on Ng non-linearly

Since Ng is a scaffolding molecule and its presence is expected to decrease $[CaM]_{free} : [Ca^{2+}]_{free}$ ratio we first decided to investigate how it affects the phosphorylation of CaMKII at different $[CaM]$ while keeping $[Ca^{2+}]$ constant. Following Pepke et al [53] we set $[CaMKII] = 80$ µM and looked at the dose response to calmodulin at $[Ca^{2+}] = 10$ µM with and without Ng. When present the concentration of Ng was set to 20 µM [73].

Since CaMKII phosphorylation depends on CaM, and the activity of the latter depends on how many Ca^{2+} ions it binds, we first look at representations of different Ca^{2+}/CaM species depending on [CaM]. Figure 2 depicts the maximum amounts of each individual Ca^{2+}/CaM species relative to total CaM available for a range of [CaM]s. We see that without Ng we consistently have more $1Ca^{2+}/CaM$ than in the presence of Ng (Figure 2a, and e top). This is easily understandable: Ng limits the availability of free calmodulin, and thus without it we have more CaM available to bind calcium. On the other hand, when we look at CaM species that have multiple calcium ions bound to them we see a crossover of the 2 curves as the total [CaM] increases. This is particularly well visible for $3Ca^{2+}/CaM$ and $4Ca^{2+}/CaM$ (Figures 2c, d and e bottom). For these species limiting the available free CaM can be beneficial since this increases the ratio $[Ca^{2+}] : [CaM]_{free}$ resulting in higher number of calmodulin proteins bound to multiple calcium ions. Figure 2e shows the dose response in the physiological range of CaM concentration. This might seem like a small effect, but it is amplified by the fact that these multi-calcium-bound calmodulin species have a higher CaMKII binding rate, and render the bound CaMKII more susceptible to phosphorylation (Table 1). We next investigate this effect.

When we look at phosphorylated CaMKII bound to different species of calmodulin, we see that Ng has very different effects on these different species (Figure 3). Phosphorylation by 1- and 2- Ca^{2+}/CaM in the presence of Ng is either lower than that in the absence of Ng (lower [CaM]) or, when the amount of CaM available is so high that the presence of Ng does not make a significant difference, the same (higher [CaM]) (Figures 3a, b, and e top 2). The situation is quite different for 3- and more importantly 4- Ca^{2+}/CaM species (Figures 3c, d and e bottom 2). At slightly higher [CaM] the competition with Ng for free CaM plays an important role: more of CaM molecules have 4 calcium ions bound to them in the presence of Ng than in the absence as discussed in the previous paragraph, and these CaM molecules give a much higher phosphorylation rates to the CaMKII monomers that they bind. However, these species only exist at relatively lower [CaM]s: as [CaM] increases the ratio $[Ca^{2+}] : [CaM]_{free}$ decreases, the effect of Ng is insubstantial at these concentrations and the 1- and 2- Ca^{2+}/CaM species are responsible for CaMKII phosphorylation. Again we show the dose response in the physiologically relevant range of [CaM] on Figure 3e. Interestingly this is where the influence of Ng is most prominent.

The dose response of total CaMKII phosphorylation to CaM is depicted on Figure 4a. Here

the first local maximum is caused by phosphorylation of the CaMKII monomers bound to $4-Ca^{2+}/CaM$, and since there is more of these species in the presence of Ng, this peak is more prominent when Ng is present in the simulations. The second peak is caused by phosphorylation of the CaMKII monomers bound to 1- and 2- Ca^{2+}/CaM which play an important role at higher [CaM] where the role of Ng is less important, and so the 2 curves overlap more and more, as the [CaM] is increased. The implications of this result can be understood by comparing Figures (4b and c) which show the dynamics of CaMKII phosphorylation with and without Ng at 2 distinct [CaM]s. These 2 values are an average (30 µM) and an upper bound to physiological (100 µM) CaM concentrations. As we can see, the effect of Ng is reversed in case of these 2 CaM concentrations: when $[CaM] = 30$µM Ng increases CaMKII phosphorylation level, and when $[CaM] = 100$µM it decreases the overall phosphorylation. Thus Ng affects the CaMKII phosphorylation dose response to CaM in a non-linear manner, that can only be clearly understood examining its effect on Ca^{2+}/CaM species and their ability to activate CaMKII.

3.2 Ng modulates mCaMKII phosphorylation in response to a Ca^{2+} spike

In the dendritic spines, the steady state calcium concentration is $\sim 100nM$ [59]. During an EPSP or an action potential, NMDA receptors in the PSD and voltage gated calcium channels (VGCC) throughout the spine briefly open letting in extracellular Ca^{+2}, which is rapidly buffered in the spine, so that $[Ca^{2+}]_{free}$ falls back to near steady state levels within ~ 100 ms [23]. So we decided to look at the CaMKII phosphorylation level not in constant high $[Ca^{2+}]$, but in more realistic conditions, where there is a spike of $\sim 10\mu M$ calcium, which is rapidly buffered [72, 19, 55, 3]. To create an accurate model, the Ca^{2+} spike should be such, that at its peak $[Ca^{2+}]_{free} \approx 10$ µM, this would better mimic the experimental results since the reported $[Ca^{2+}]$ is the concentration of free calcium, and not that of the total calcium influx which is higher and is quickly buffered by Ca^{2+} binding proteins [46, 3]. For this purpose we found, through trial and error, the concentration of Ca^{2+} influx at the peak, in the absence of any Ca^{2+}-binding molecules should reach $\sim 25-145$ µM, depending on the presence of Ng and $[CaM]$, so that in our simulated conditions $[Ca^{2+}]_{free} = 10$ µM at the peak. Note that this is not representative of the actual amount of calcium ions entering the spine, since our model does not include any of the calcium binding molecules (with the exception of calmodulin), and only simulates calcium buffering mathematically. For our simulation purposes however the calcium signal which mimics that measured experimentally is all that matters.

Before simulating the calcium spike we allow the system to equilibrate. There is some basal level of CaMKII phosphorylation even at the low calcium concentrations (~ 100 nM) observed in the spine in equilibrium. Again the important parameter here is the $[Ca^{2+}]_{free}$, since this is what is measured experimentally. To achieve a given $[Ca^{2+}]_{free}$ in different conditions the concentration of total calcium varies depending on the conditions simulated, and so does the basal CaMKII phosphorylation level. To enable direct comparison we look at the difference of the peak and basal phosphorylation for each condition, as well as the Area Under the Curve (AUC), peak time, and

the decay time of phosphorylation levels.

We first decided to look at maximum CaMKII phosphorylation dependence on the amplitude of the Ca^{2+}_{free} pulse. On Figure 5 the horizontal axis represents the "measured" $[Ca^{2+}]_{free}$ and the vertical axis shows the level of maximal CaMKII phosphorylation. As we can see in this case for any $[Ca^{2+}]_{free}$ the response is higher in the absence of Ng, indicating that even for very small $[Ca^{2+}]$ spikes, the availability of CaM is the limiting factor for CaMKII phosphorylation. This is further confirmed by the fact that as the size of the Ca^{2+} spike increases the two curves diverge further as they reach saturation.

The dynamics of CaMKII phosphorylation is shown on Figure 6a for a range of physiological CaM concentrations including the upper limit of 100 µM. As we can see, even in this extreme case Ng decreases CaMKII phosphorylation, indicating the [CaM] is the limiting factor. Interestingly, the phosphorylation dynamics with Ng and at 50M [CaM] is identical to that without Ng at 30 µM [CaM].

Further comparing the total amount of CaMKII phosphorylation over time (Area Under the Curve or AUC) as well as the relative peak phosphorylation levels (Figures 7a, top and b), we see that Ng makes a striking difference: it's presence dramatically impairs phosphorylation of CaMKII. However, at extreme high [CaM] (100µM) the system is robust to the presence of Ng although the latter still modulates the level of phosphorylation. The presence of Ng does not appear to have a dramatic effect on the peak time or phosphorylation lifetime, which we define as the time it takes to reach down to 10% of the peak phosphorylation level, for tested calmodulin concentrations (Figures 7e, and g). This is expected; once phosphorylated, the CaMKII molecules can be dephosphorylated by PP1, which works independent of Ng (and in our model, of any other molecule).

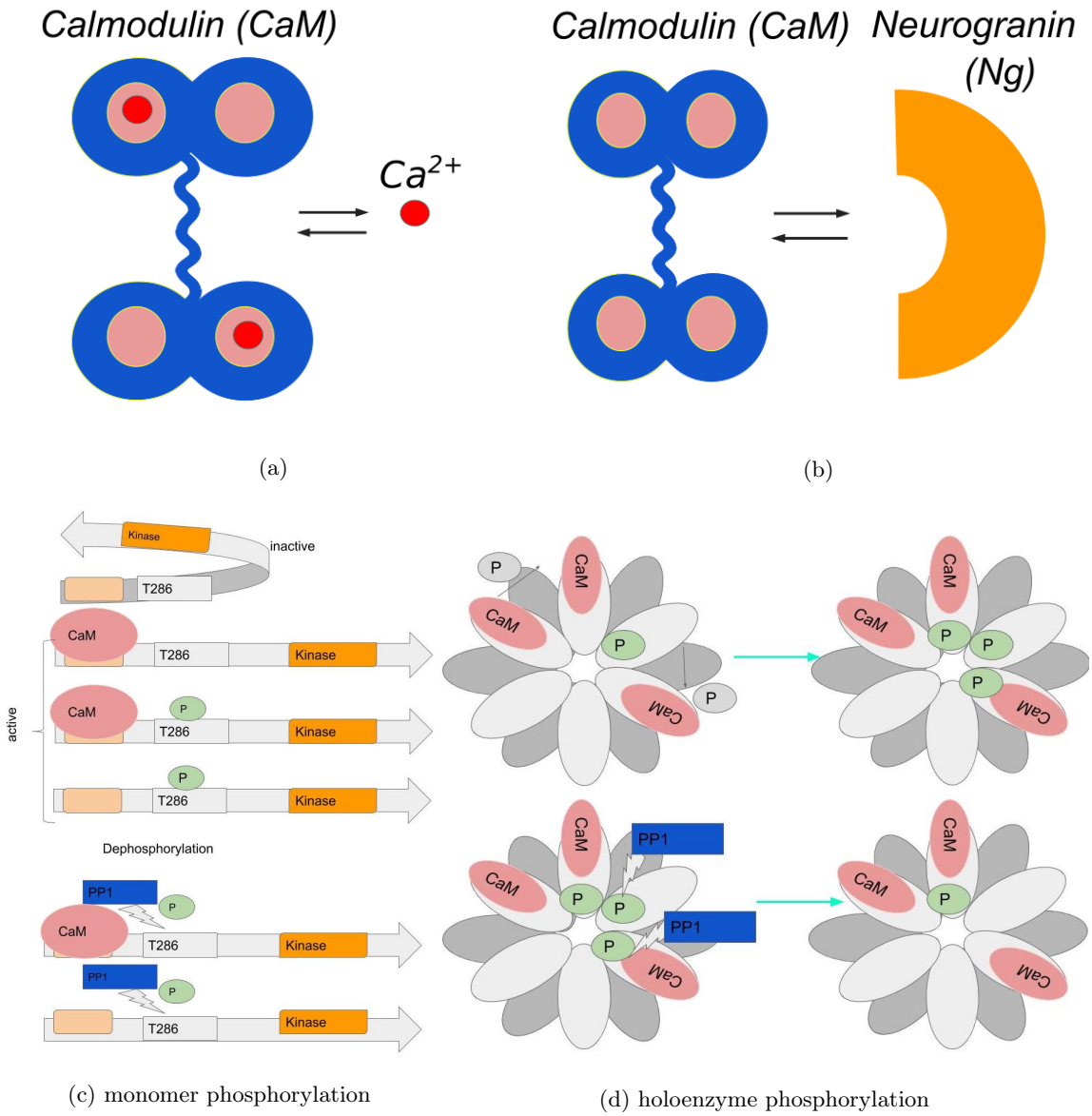

Figure 1: Schematic representation of the interactions between calmodulin (CaM), calcium, CaMKII, and neurogranin (Ng) (a) Calmodulin has 4 calcium binding sites; it binds Ca^{2+} cooperatively and its ability to activate CaMKII depends on how many of these sites are occupied. (b) Neurogranin (Ng) is a scaffolding molecule; upon binding calmodulin dramatically reduces it's affinity for calcium. In this work, we assume that CaM cannot bind calcium and Ng simultaneously. (c) The default conformation of CaMKII monomers is inactive (top); they can be activated by CaM binding. Once bound to CaM, the monomers can be phosphorylated by another active CaMKII protein. In this case, the CaMKII monomer will remain active even after losing CaM. Protein phosphatase 1 (PP1) dephosphorylates CaMKII (bottom). (d) CaMKII holoenzyme is a dodecamer, which consists of 2 stacked hexomeric rings of CaMKII monomers. Within the ring, a given CaMKII monomer can be phosphorylated by its neighbor provided that they are both in the active conformation. This is commonly referred to as autophosphorylation.

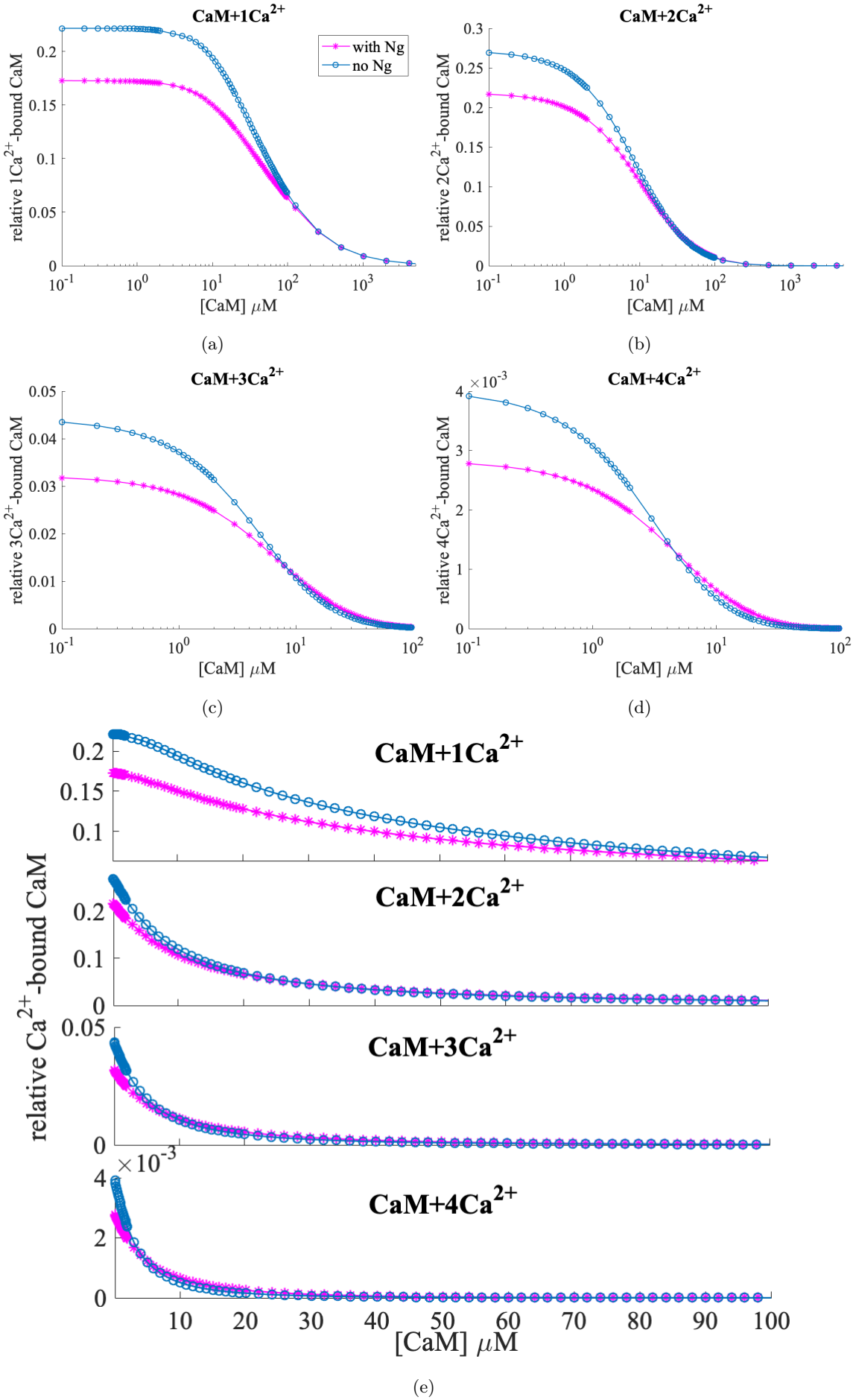

Figure 2: Relative concentration of (a) 1-,(b) 2-, (c) 3- and (d) 4-calcium-bound calmodulin vs. total [CaM]. For most of the calcium-bound forms, the relative concentration is lower in the presence of neurogranin. However, in the case of 3- and 4-calcium-bound calmodulin the situation is reversed for certain [CaM]: Ng competes with Ca^{2+} for free calmodulin, which allows a regime where the concentration of these "multi-calcium-bound" forms is higher. As the concentration of calmodulin is further increased, the ratio $[Ca^{2+}] : [CaM]$ decreases and these forms die out, thus at high [CaM] the effects of Ng are diminished. (e) shows the same effect in physiologically relevant [CaM].

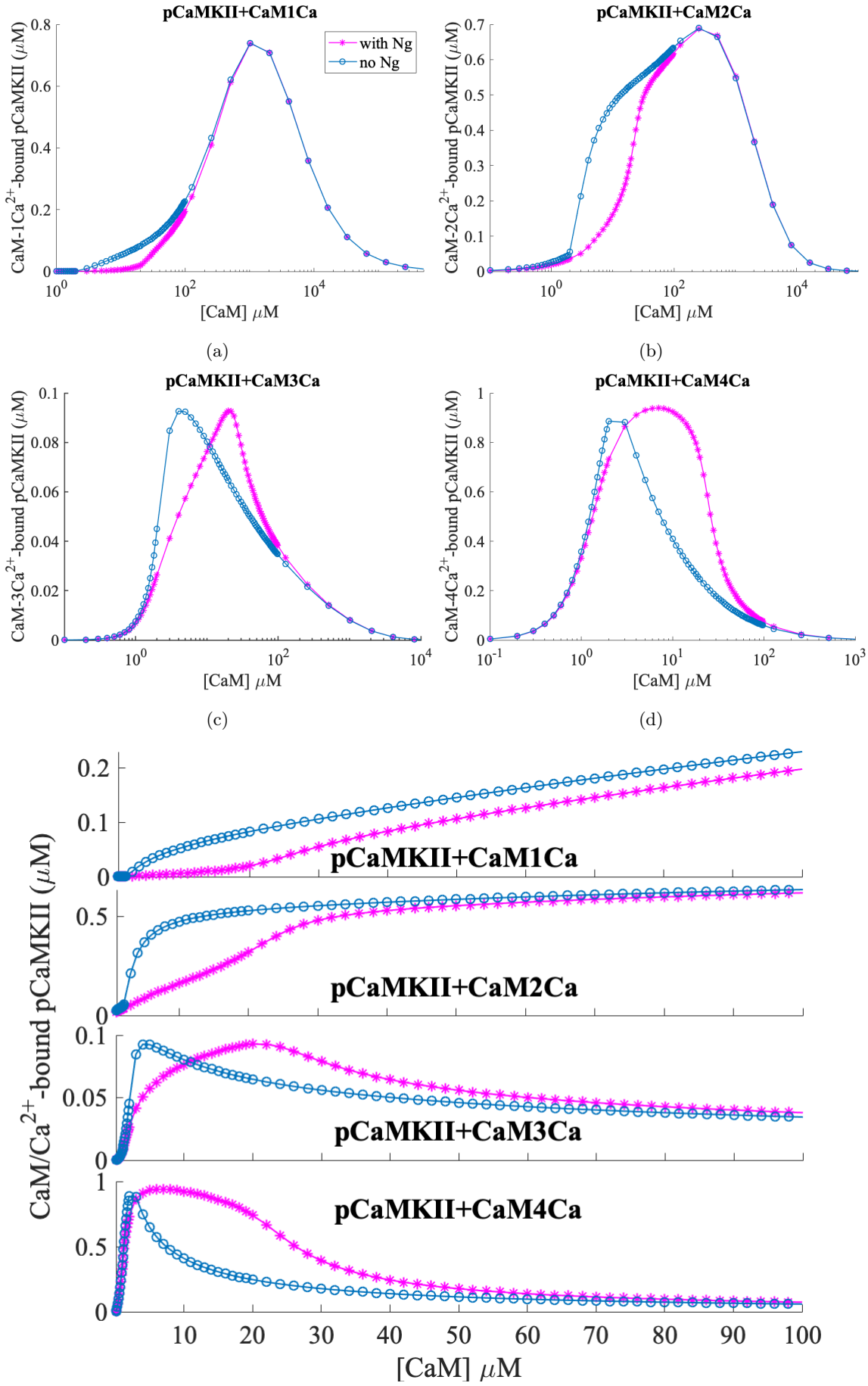

Figure 3: Dose response of phosphorylated CaMKII molecules bound to different states of CaM-Ca^{2+} as shown on Figure 2. At low [CaM], the "multi-calcium-bound" forms of calmodulin play an important role. This is amplified by the fact that these forms when bound to CaMKII give it higher phosphorylation rates (Table 1).

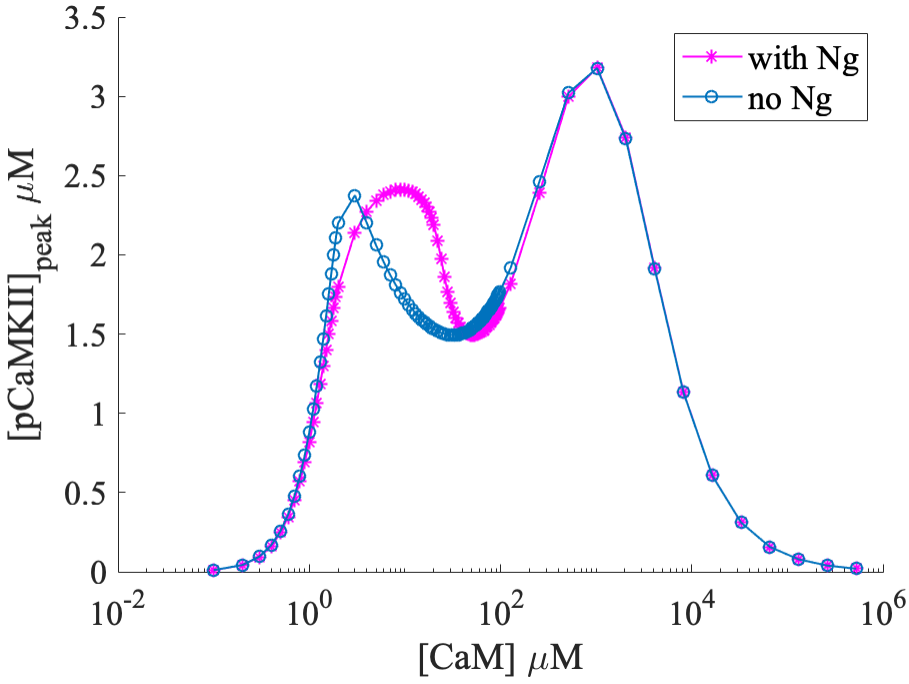

(a)

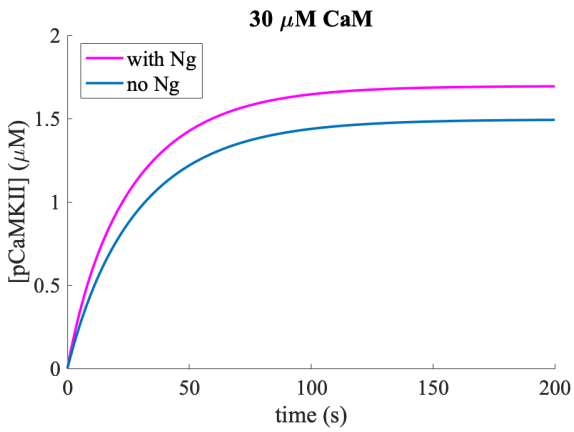

(b)

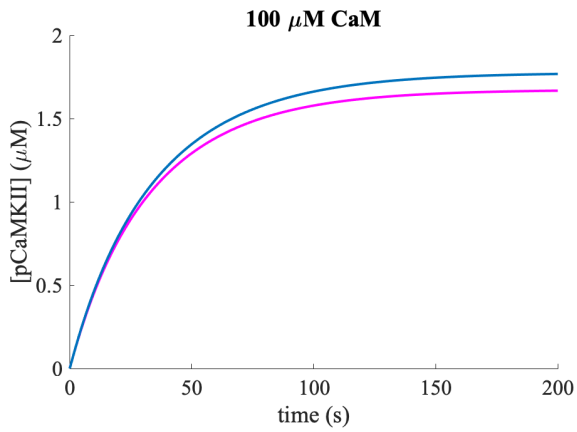

(c)

Figure 4: CaMKII phosphorylation dependence on [CaM] and Ng. (a) Steady state phosphorylated CaMKII concentration as a function of total CaM concentration in the presence of 10µM Ca^{2+} with (pink lines) and without Ng (blue lines). (a) and (b) Dynamics of CaMKII monomers (80 µM) autophosphorylation and dephosphorylation by PP1, in the presence of constant $[Ca^{2+}] = 10$µM with and without neurogranin, with $[CaM] = 30$ µM and $[CaM] = 100$ µM respectively.

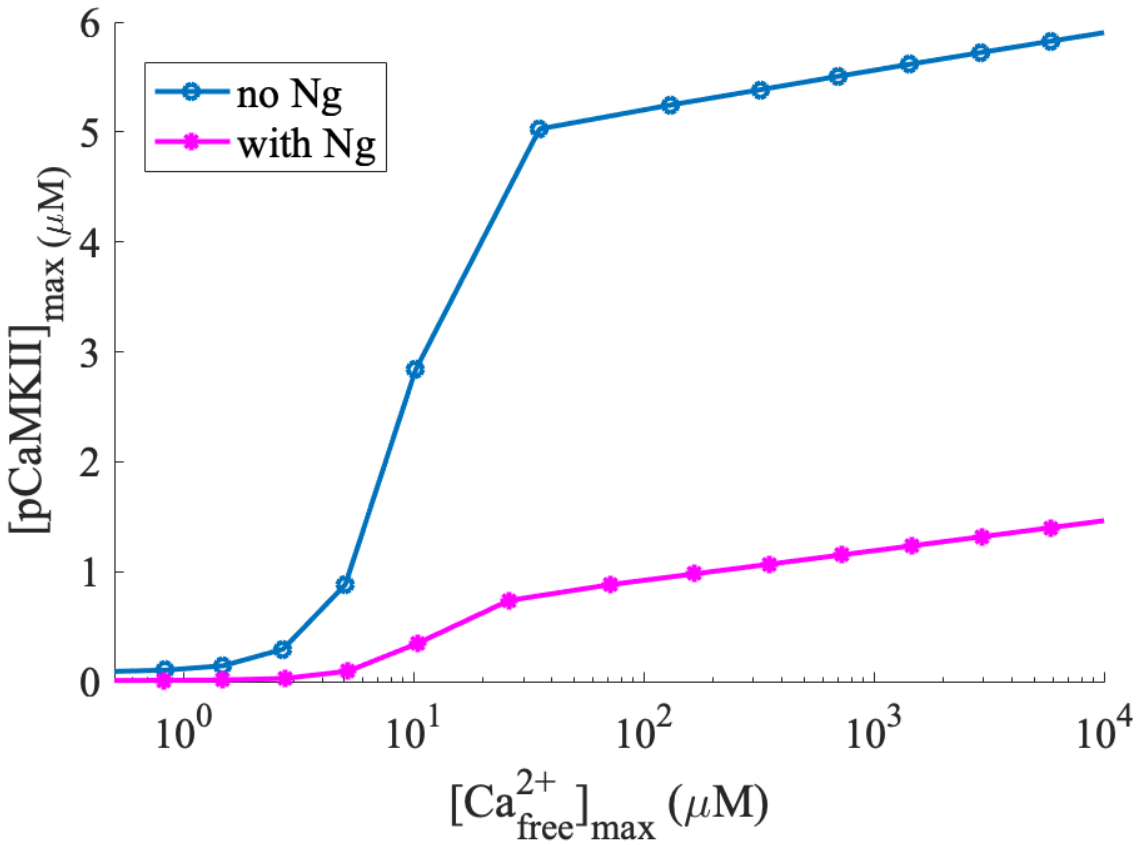

Figure 5: Maximum phosphorylated CaMKII concentration for different concentrations of Ca^{2+} spikes with [CaM] = 30 µM. The horizontal axis represents the free calcium available at the peak of the spike.

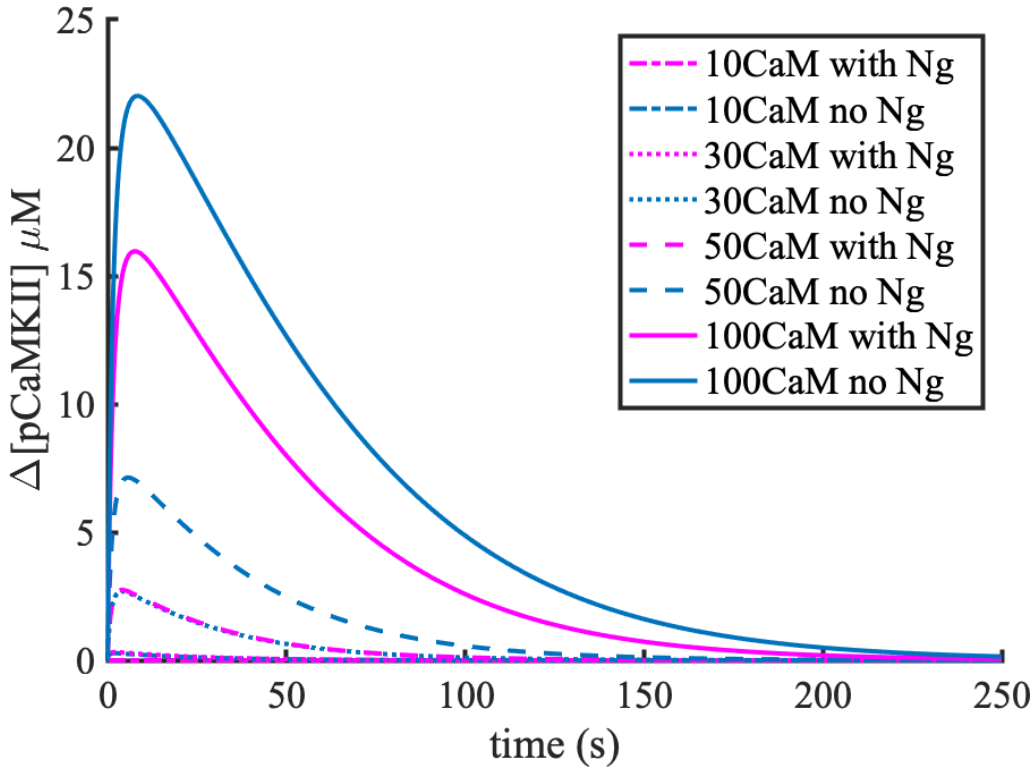

(a)

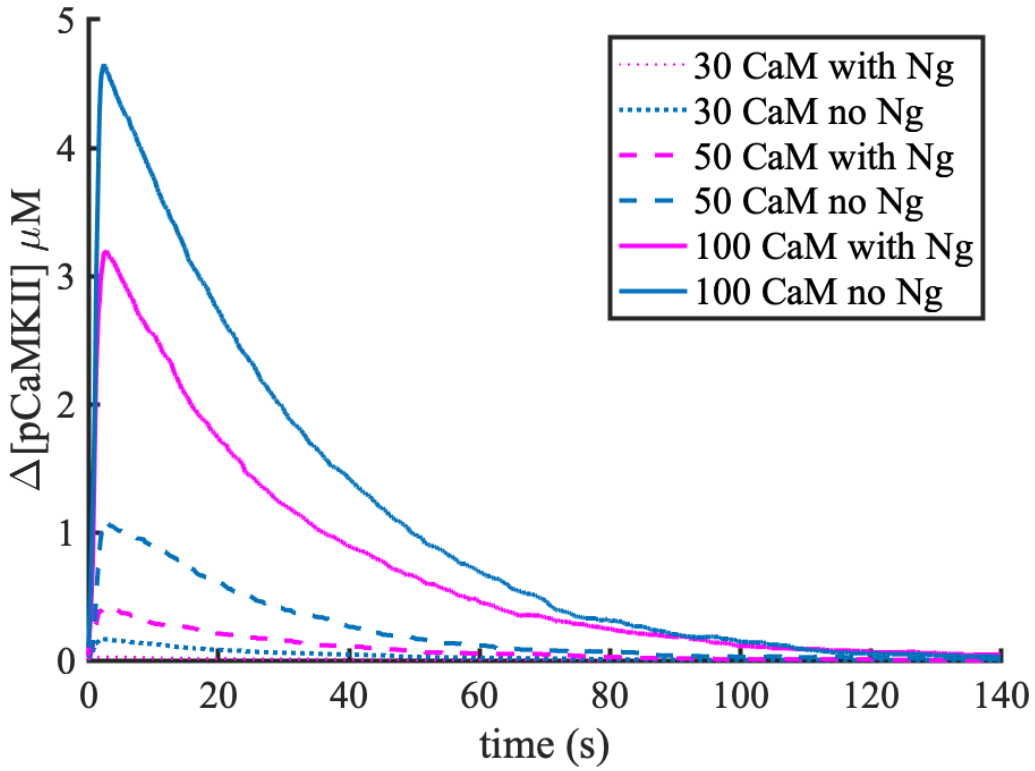

(b)

Figure 6: The rise in CaMKII phosphorylation level as a response to a $[Ca^{2+}]_{free} = 10$ µM spike with monomers (a) and holoenzymes (b) for different conditions. The response of the holoenzyme at [CaM] = 10 µM was not significant and is not shown here.

3.3 CaMKII holoenzyme phosphorylation is robust against fluctuations of $[Ca^{2+}]_{free}$

After thoroughly investigating the behaviour of CaMKII monomers through our simulations we are now ready to move on and characterize the behavior of the holoenzyme. As discussed above the holoenzyme has too many possible states, and therefore this case is not feasible to solve analytically, and we adopted a stochastic agent-based approach.

Figures 6b shows the average CaMKII phosphorylation in response to a $\sim$ 10 µM single Ca^{2+} spike for $[CaM] = 30\mu M, 50\mu M$ and $100\mu M$ respectively. We also conducted simulations in at $[CaM] = 10\mu M$ however at this CaM concentration CaMKII did not react to 10 µM Ca^{2+} pulses. Since this simulations were stochastic the results had to be averaged. In the simulations with $[CaM] = 30$µM the mean peak and standard deviation of $[Ca^{2+}]_{free}$ were 10.7 ± 1.6µM in the case with no Ng and 10.3 ± 1.2µM in the case with Ng. We note, that with this [CaM] the CaMKII would not always react to the 10 M free calcium spike, and sometimes there would be no detected phosphorylated CaMKII. These measurements were not taken into account in the calculations plotted on Figures 6b and 7b, d, f and g. For the model with Ng we had to conduct 120 simulations out of which only 31 resulted in noticeable CaMKII phosphorylation, and without Ng 36 out 60 simulations yielded change in phosphorylation levels. When $[CaM] = 50$µM the average Ca pulse was the mean peak and standard deviation of $[Ca^{2+}]_{free}$ were 9.4 ± 1.2µM in the case with no Ng and 10.2 ± 1.3µM in the case with Ng. Finally in the extreme case when $[CaM] = 100$µM the corresponding numbers were 9.2 ± 1.3µM both with and without Ng.

By comparing the Figures 6a and b, 7a, c, e and b, d and f we notice that with the same amount of CaM present in the simulation the holoenzyme reacts significantly faster to the calcium signal (see the peak time), however the phosphorylation level is also much lower. This tells us that the holoenzyme is more robust against Ca^{2+} fluctuations. When it does react to a calcium signal however the phosphorylation lifetime is comparable to that of the monomers (Figures 7g and h). And as in the case for monomers the presence of neurogranin modulates the effect of the calcium signal at physiological calmodulin concentrations.

3.4 A leaky integrator of $[Ca^{2+}]$ signals

Since in *in vivo* experiments, the usual protocol for observing CaMKII phosphorylation involves inducing a train of Ca^{2+} spikes [24, 66, 36, 14] we decided next to look at a simulation of multiple calcium spikes in our model. Figure 8 shows the average response of CaMKII phosphorylation

to 10 calcium pulses at 0.5 Hz. As we can see, even with 10 Ca^{2+} pulses in the case of $[CaM] = 30\mu M$ the response is very small, particularly in the presence of Ng. In fact, even with 10 calcium pulses only 25 out of 30 simulations resulted in a non-negligible difference of CaMKII phosphorylation levels in the presence of Ng, and only 28 out of 30 in the absence of Ng.

As before the presence of Ng makes less of a difference when the concentration of calmodulin is higher (100 µM), and this system is far more sensitive to calcium signals (Figures 8a, c and d). We also decided to look at the ratios of the CaMKII phosphorylation metrics (namely area under the curve and maximum change in phosphorylation) for 10 to 1 calcium pulses. This ratios are shown on Figure 8b for all 6 conditions tested. As can be seen here, for average physiological conditions a 10-fold increase in Ca^{2+} signal results in a more modest increase in CaMKII phosphorylation. With the exception of 100 µM (ultrahigh) CaM concentration the ratio of the changes in phosphorylated CaMKII concentrations is consistently lower than 10, and even the ratios of AUCs get close to 10 only for [CaM] = 50 µM in the absence of Ng. This indicates a leakage in the process of the calcium signal integration. This prediction of our model recently been observed experimentally *in vivo* [14].

To further investigate this process we looked at CaMKII phosphorylation in response to 30 Ca^{2+} pulses (Figures 9) at average physiological [CaM]. From Figure 9a we can clearly see that the rate of increase in phosphorylation level decreases as more calcium pulses are added. This leakage of the calcium signal integration is caused by dephosphorylation of CaMKII by PP1.

As mentioned previously, the holoenzyme phosphorylation curves discussed until now are results of averaging multiple runs of given models. Since these simulations are conducted stochastically, the timing of Ca^{2+} signals is also stochastic, and not exactly synchronized across the multiple runs. Figure 9b shows CaMKII phosphorylation in response to a train of 0.5 Hz Ca^{2+} pulses for 3 individual runs. We see that the phosphorylation level raises in a stepwise manner in response to each calcium spike.

To better characterize CaMKII as a leaky integrator and the effect Ng has on it we fit the CaMKII phosphorylation curves at a physiological $[CaM] = 30\mu M$ to the equation $x = k - k \cdot e^{-a \cdot t}$ where k is the maximum possible change of phosphorylation level and a is the overall phosphorylation rate (Figure 7c). The curve fitting tool from *MATLAB* was used for this purpose. The response with Ng was characterized by the equation $0.36 - 0.36 \cdot e^{-0.045 \cdot t}$ with an $R^2 = 0.9683$ and the response without Ng by $7.24 - 7.24 \cdot e^{-0.025 \cdot t}$ with an $R^2 = 0.9979$. This result demonstrates that Ng not only regulates the leaking rate of the integrator, but also severely reduces the maximum possible phosphorylation level. The results on Figures 8 and 9

predict that our model behaves as a leaky integrator of calcium signals, and that the presence of Ng dramatically affects the properties of this integrator.

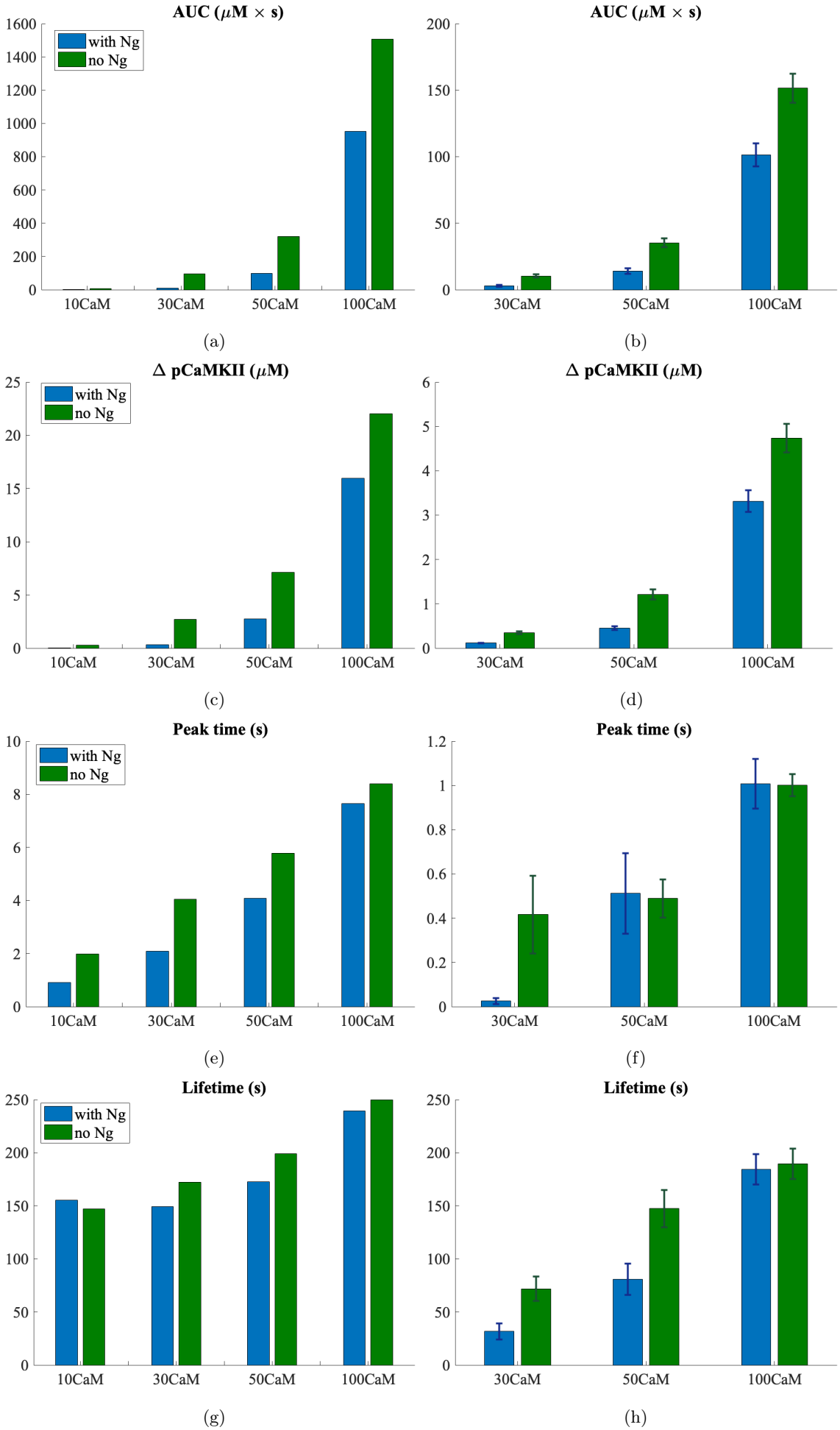

Figure 7: Bar graphs in different conditions for the monomers and holoenzymes respectively of Area Under the Curve (AUC) (a) and (b), the maximum increase in phosphorylated CaMKII concentration (c) and (d), the time of the phosphorylation level reaching its peak (e) and (g) the lifetime defined in the main text (g) and (h) in response to a 10 µM Ca pulse.

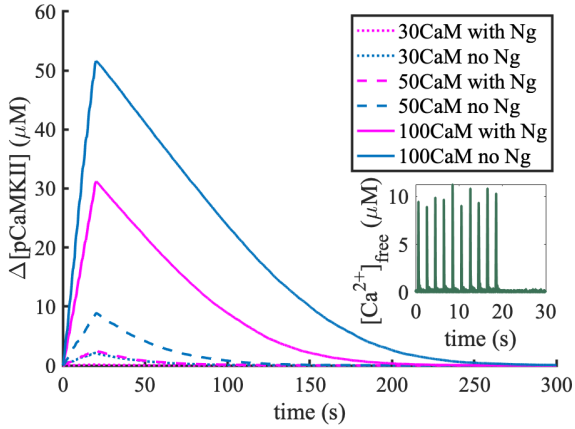

(a)

Conditions	$\frac{AUC_{10}}{AUC_1}$	$\frac{\Delta pCaMKII_{10}}{\Delta pCaMKII_1}$
30 CaM with Ng	2.2 ± 0.6	1.7 ± 0.5
30 CaM no Ng	7.8 ± 1.1	6.3 ± 0.3
50 CaM with Ng	6.6 ± 1	5.7 ± 1.4
50 CaM no Ng	11.4 ± 1.1	7.4 ± 0.3
100 CaM with Ng	21.2 ± 6.3	9.5 ± 0.7
100 CaM no Ng	31.2 ± 2.4	10.9 ± 0.8

(b)

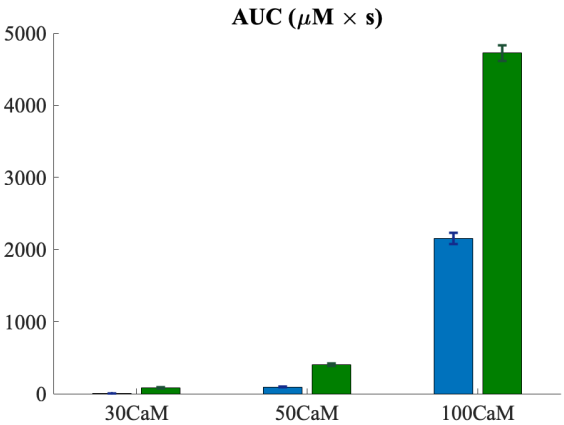

(c)

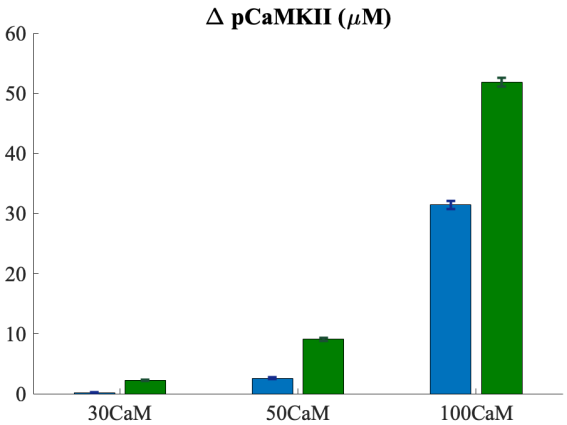

(d)

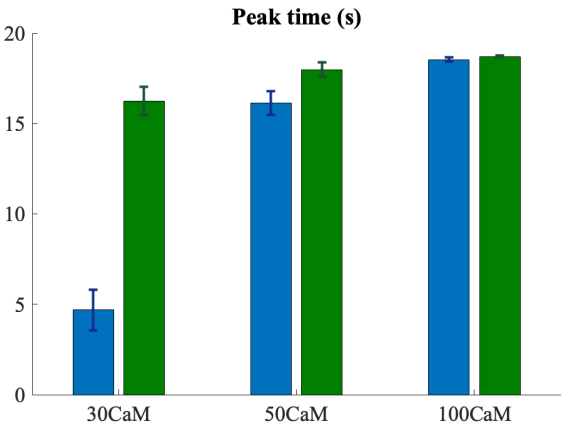

(e)

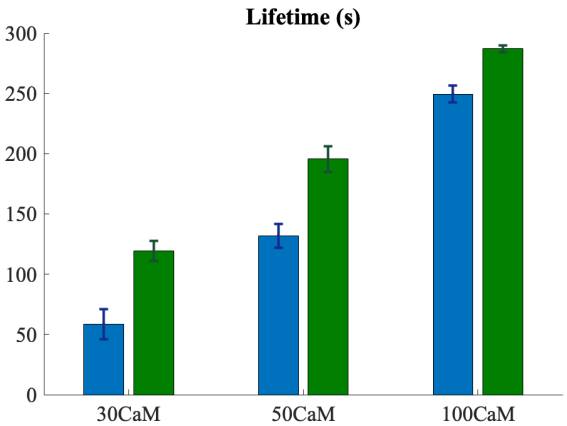

(f)

Figure 8: (a) An average phosphorylation of CaMKII holoenzyme in response to 10 Ca pulses at 0.5 Hz averaged over 30 simulations with 63 holoenzymes and 30 µM 50 µM, and 100 µM calmodulin. Bar graphs comparing the (b) the ratios of the Area under the curve and maximum change in phosphorylation level in response to 10 and 1 Ca pulses in different conditions. (c) Area Under the Curve (AUC), (d) the maximum increase in the CaMKII phosphorylation concentration, (e) the time of the phosphorylation level reaching its peak, and (f) the lifetime defined in the main text for in response these Ca^{2+} pulses.

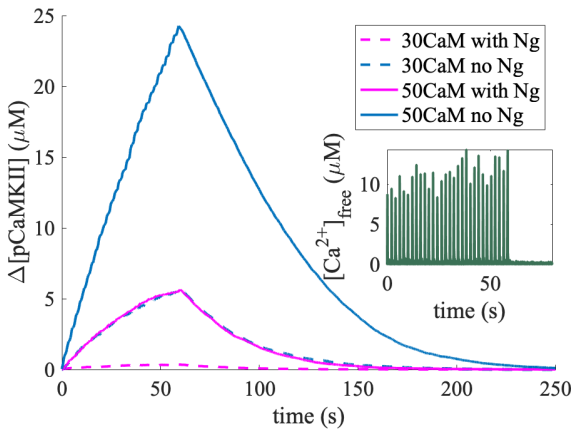

(a)

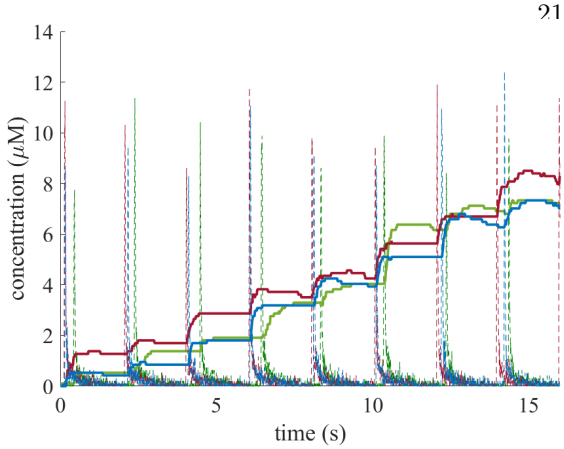

(b)

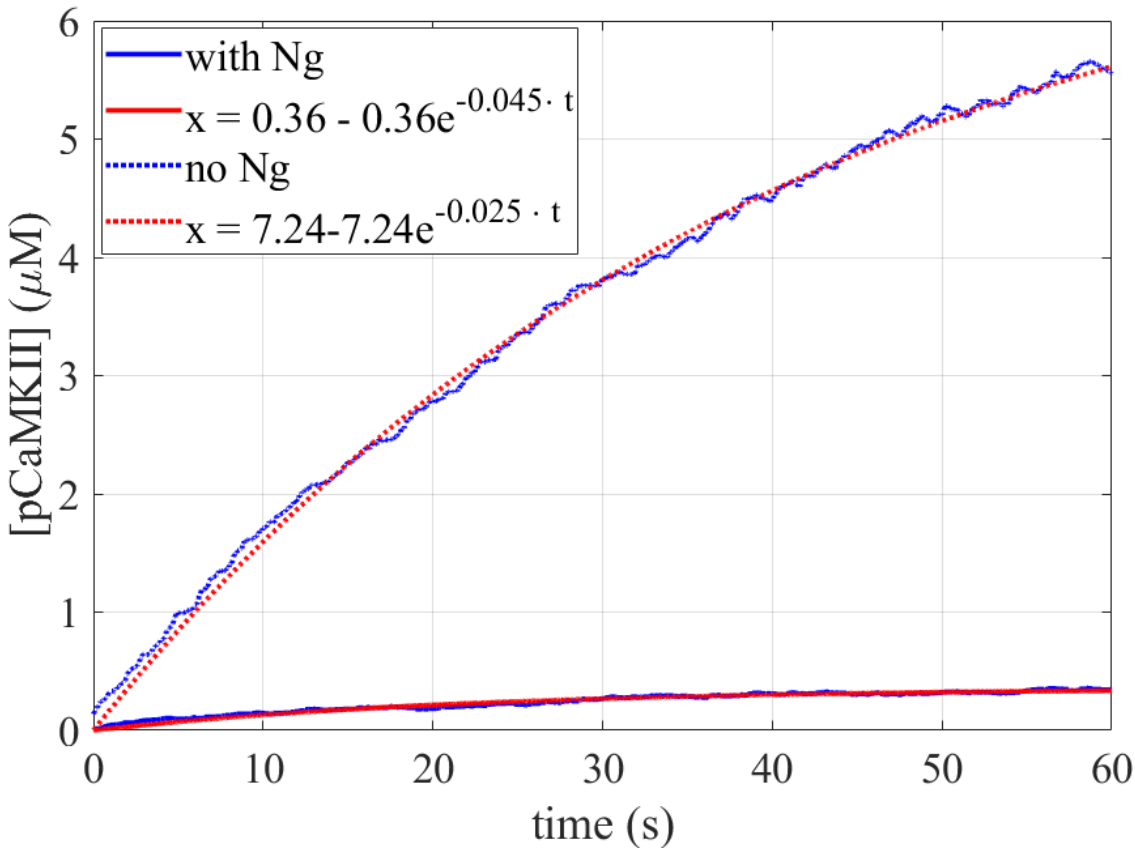

(c)

Figure 9: (a) An average phosphorylation of CaMKII holoenzyme in response to 30 Ca pulses at 0.5 Hz averaged over 30 simulations with 63 holoenzymes and 30 µM, and 50 µM) calmodulin. (b) Three individual simulations: the response of CaMKII phosphorylation level (solid lines) change to the calcium spikes (dashed lines).(c) Fitting the leaky integrator. The average response to 30 Ca^{2+} pulses was fitted to a curve of the form $x = k - k \cdot e^{-a \cdot t}$ with and without Ng and $[CaM] = 30$µM, with the curve fitting tool from MATLAB. The parameters obtained are: $k = 7.24, a = 0.025$ with an $R^2 = 0.9979$ without Ng and $k = 0.36, a = 0.045$ with an $R^2 = 0.9683$ with Ng. Thus Ng not only changes the leaking rate of the integrator, but significantly lowers the maximum possible phosphorylation level.

4 Discussion

In this paper we started out with replicating the results from Pepke et al [53] for monomeric CaMKII in the presence of constant $[CaM] = 30$µM and $[Ca^{2+}] = 10$µM.

We then added $[Ng] = 20$µM to our simulation to investigate the effect of this scaffolding protein on mCaMKII phosphorylation. We discovered that under the investigated conditions Ng affects mCaMKII phosphorylation dose-response to CaM in a non-linear manner. To better understand this effect we looked at individual CaM/Ca^{2+} species as well as phosphorylated CaMKII monomers bound to these species. The sum of these species mirrors the dose response overall CaMKII phosphorylation, which shows importantly, that the effect of Ng on this curve is most pronounced at $[CaM] = 10 - 100$µM which is the physiological [CaM] concentration at dendritic spines.

The next step we took was decreasing the constant $[Ca^{2+}]$ to 100 nM, and investigating the phosphorylation in response to a measured $[Ca^{2+}] = 10$µM pulse in the presence of a phosphatase PP1, which more closely mimics the physiological conditions. We found that in this case the scaffolding molecule Ng modulates CaMKII phosphorylation in response to a Ca^{2+} signal, and this effect is higher at average physiological [CaM] (30 - 50 µM) and lower, but still present, at the extreme high concentration (100 µM).

Finally, we moved on to investigate the dodecameric holoenzyme of CaMKII and the dynamics of its phosphorylation in response to $[Ca^{2+}]$ signals. What we discovered was that the holoenzyme is more robust against free $[Ca^{2+}]$ fluctuations, particularly at physiological [CaM] (30 - 50 µM). Our most important result was to show that the CaMKII-CaM-PP1 system behaves as a leaky integrator of calcium signals. We were able to quantitatively characterize this integrator as well as the modulating effect of Ng on this system.

Phosphorylation of CaMKII activates its kinase domain which leads to subsequent modification of the dendritic spine and the postsynaptic density. Specifically it unbinds from F-actin inside of the spine allowing reorganization of the cytoskeleton, and rebinds this newly structured F-actin after it has been dephosphorylated [60, 71, 22, 68, 13]. CaMKII activation also leads to trafficking [74, 50] and trapping [1] of AMPA receptors at the PSD as well as an increase in these receptors conductance after the induction of LTP [2, 5, 35, 33]. All of this in turn results in change of size and strength of the synapse (Figure 10).

It has been shown that synaptic size and strength are regulated by firing history [7] with very high precision [4]. As a synapse undergoes more LTP it grows larger and subsequently the Ca^{2+}

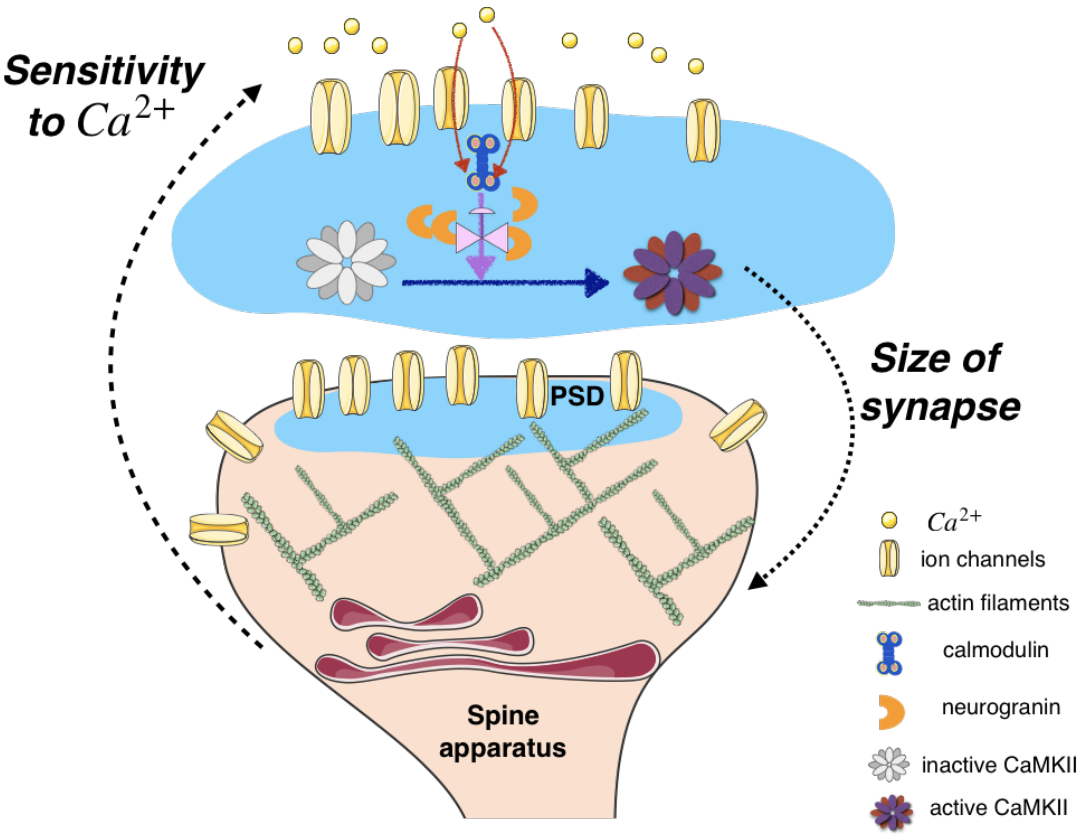

Figure 10: Schematic representation of CaMKII phosphorylation controlling sensitivity of a synapse to Ca^{2+} signals.

transients in this spines become more dilute in response to back-propagating action potentials [3]. Thus we can say that integration of Ca^{2+} signals is an in-built mechanism in the dendritic spine to down-regulate its sensitivity to these signals as the corresponding synapse grows larger. This is schematically depicted on Figure 10.

5 Acknowledgments

We thank Miriam Bell for useful discussions and assistance with making figure 10. We also thank Donya Ohadi and Andrea Cugno for useful discussions. This work was supported by the following grants: FA9550-18-1-0051 (PR,MO,TB,TS), NIH: P41GM103712 (TS,TB,MO), NS44306 (MK,TB,TS), DA030749 (MK,TB,TS).

References

[1] V. J. Appleby, S. A. Corrêa, J. K. Duckworth, J. E. Nash, J. Noël, S. M. Fitzjohn, G. L. Collingridge, and E. Molnár. Ltp in hippocampal neurons is associated with a camkii-mediated increase in glua1 surface expression. *Journal of neurochemistry*, 116(4):530–543, 2011.

[2] A. Barria, D. Muller, V. Derkach, L. C. Griffith, and T. R. Soderling. Regulatory phosphorylation of ampa-type glutamate receptors by cam-kii during long-term potentiation. *Science*, 276(5321):2042–2045, 1997.

[3] T. M. Bartol, D. X. Keller, J. P. Kinney, C. L. Bajaj, K. M. Harris, T. J. Sejnowski, and M. B. Kennedy. Computational reconstitution of spine calcium transients from individual proteins. *Frontiers in synaptic neuroscience*, 7:17, 2015.

[4] T. M. Bartol Jr, C. Bromer, J. Kinney, M. A. Chirillo, J. N. Bourne, K. M. Harris, and T. J. Sejnowski. Nanoconnectomic upper bound on the variability of synaptic plasticity. *Elife*, 4:e10778, 2015.

[5] T. A. Benke, A. Lüthi, J. T. Isaac, and G. L. Collingridge. Modulation of ampa receptor unitary conductance by synaptic activity. *Nature*, 393(6687):793, 1998.

[6] M. K. Bennett, N. E. Erondu, and M. B. Kennedy. Purification and characterization of a calmodulin-dependent protein kinase that is highly concentrated in brain. *Journal of Biological Chemistry*, 258(20):12735–12744, 1983.

[7] G.-q. Bi and M.-m. Poo. Synaptic modifications in cultured hippocampal neurons: dependence on spike timing, synaptic strength, and postsynaptic cell type. *Journal of neuroscience*, 18(24):10464–10472, 1998.

[8] M. L. Blinov, J. R. Faeder, B. Goldstein, and W. S. Hlavacek. Bionetgen: software for rule-based modeling of signal transduction based on the interactions of molecular domains. *Bioinformatics*, 20(17):3289–3291, 2004.

[9] J. Borovac, M. Bosch, and K. Okamoto. Regulation of actin dynamics during structural plasticity of dendritic spines: Signaling messengers and actin-binding proteins. *Molecular and Cellular Neuroscience*, 2018.

[10] J. M. Bradshaw, A. Hudmon, and H. Schulman. Chemical quenched flow kinetic studies indicate an intraholoenzyme autophosphorylation mechanism for ca2+/calmodulin-dependent protein kinase ii. *Journal of Biological Chemistry*, 277(23):20991–20998, 2002.

[11] J. M. Bradshaw, Y. Kubota, T. Meyer, and H. Schulman. An ultrasensitive ca2+/calmodulin-dependent protein kinase ii-protein phosphatase 1 switch facilitates specificity in postsynaptic calcium signaling. *Proceedings of the National Academy of Sciences*, 100(18):10512–10517, 2003.

[12] S. E. Brown, S. R. Martin, and P. M. Bayley. Kinetic control of the dissociation pathway of calmodulin-peptide complexes. *Journal of Biological Chemistry*, 272(6):3389–3397, 1997.

[13] H. J. Carlisle, P. Manzerra, E. Marcora, and M. B. Kennedy. Syngap regulates steady-state and activity-dependent phosphorylation of cofilin. *Journal of Neuroscience*, 28(50):13673–13683, 2008.

[14] J.-Y. Chang, P. Parra-Bueno, T. Laviv, E. M. Szatmari, S.-J. R. Lee, and R. Yasuda. Camkii autophosphorylation is necessary for optimal integration of ca 2+ signals during ltp induction, but not maintenance. *Neuron*, 94(4):800–808, 2017.

[15] L. H. Chao, M. M. Stratton, I.-H. Lee, O. S. Rosenberg, J. Levitz, D. J. Mandell, T. Kortemme, J. T. Groves, H. Schulman, and J. Kuriyan. A mechanism for tunable autoinhibition in the structure of a human ca2+/calmodulin-dependent kinase ii holoenzyme. *Cell*, 146(5):732–745, 2011.

[16] R. J. Colbran. Protein phosphatases and calcium/calmodulin-dependent protein kinase ii-dependent synaptic plasticity. *Journal of Neuroscience*, 24(39):8404–8409, 2004.

[17] R. A. Copeland. *Enzymes: a practical introduction to structure, mechanism, and data analysis*. John Wiley & Sons, 2004.

[18] S. J. Coultrap and K. U. Bayer. Camkii regulation in information processing and storage. *Trends in neurosciences*, 35(10):607–618, 2012.

[19] W. Denk, R. Yuste, K. Svoboda, and D. W. Tank. Imaging calcium dynamics in dendritic spines. *Current opinion in neurobiology*, 6(3):372–378, 1996.

[20] J. R. Faeder, M. L. Blinov, and W. S. Hlavacek. Rule-based modeling of biochemical systems with bionetgen. In *Systems biology*, pages 113–167. Springer, 2009.

[21] B. E. Finn and S. Forsén. The evolving model of calmodulin structure, function and activation. *Structure*, 3(1):7–11, 1995.

[22] I. N. Fleming, C. M. Elliott, and J. H. Exton. Phospholipase c-γ, protein kinase c and ca2+/calmodulin-dependent protein kinase ii are involved in platelet-derived growth factor-induced phosphorylation of tiam1. *FEBS letters*, 429(3):229–233, 1998.

[23] K. M. Franks and T. J. Sejnowski. Complexity of calcium signaling in synaptic spines. *Bioessays*, 24(12):1130–1144, 2002.

[24] H. Fujii, M. Inoue, H. Okuno, Y. Sano, S. Takemoto-Kimura, K. Kitamura, M. Kano, and H. Bito. Nonlinear decoding and asymmetric representation of neuronal input information by camkiiα and calcineurin. *Cell reports*, 3(4):978–987, 2013.

[25] T. R. Gaertner, J. A. Putkey, and M. N. Waxham. Rc3/neurogranin and ca2+/calmodulin-dependent protein kinase ii produce opposing effects on the affinity of calmodulin for calcium. *Journal of Biological Chemistry*, 279(38):39374–39382, 2004.

[26] P. I. Hanson, M. S. Kapiloff, L. L. Lou, M. G. Rosenfeld, and H. Schulman. Expression of a multifunctional ca2+/calmodulin-dependent protein kinase and mutational analysis of its autoregulation. *Neuron*, 3(1):59–70, 1989.

[27] P. I. Hanson, T. Meyer, L. Stryer, and H. Schulman. Dual role of calmodulin in autophosphorylation of multifunctional cam kinase may underlie decoding of calcium signals. *Neuron*, 12(5):943–956, 1994.

[28] P. I. Hanson and H. Schulman. Inhibitory autophosphorylation of multifunctional ca2+/calmodulin-dependent protein kinase analyzed by site-directed mutagenesis. *Journal of Biological Chemistry*, 267(24):17216–17224, 1992.

[29] L. A. Harris, J. S. Hogg, J.-J. Tapia, J. A. Sekar, S. Gupta, I. Korsunsky, A. Arora, D. Barua, R. P. Sheehan, and J. R. Faeder. Bionetgen 2.2: advances in rule-based modeling. *Bioinformatics*, 32(21):3366–3368, 2016.

[30] M. J. Higley and B. L. Sabatini. Calcium signaling in dendritic spines. *Cold Spring Harbor perspectives in biology*, 4(4):a005686, 2012.

[31] L. Hoffman, A. Chandrasekar, X. Wang, J. A. Putkey, and M. N. Waxham. Neurogranin alters the structure and calcium-binding properties of calmodulin. *Journal of Biological Chemistry*, pages jbc–M114, 2014.

[32] A. Hudmon and H. Schulman. Neuronal ca2+/calmodulin-dependent protein kinase ii: the role of structure and autoregulation in cellular function. *Annual review of biochemistry*, 71(1):473–510, 2002.

[33] G. Krapivinsky, I. Medina, L. Krapivinsky, S. Gapon, and D. E. Clapham. Syngap-mupp1-camkii synaptic complexes regulate p38 map kinase activity and nmda receptor-dependent synaptic ampa receptor potentiation. *Neuron*, 43(4):563–574, 2004.

[34] Y. Kubota, J. A. Putkey, and M. N. Waxham. Neurogranin controls the spatiotemporal pattern of postsynaptic ca2+/cam signaling. *Biophysical journal*, 93(11):3848–3859, 2007.

[35] H.-K. Lee, M. Barbarosie, K. Kameyama, M. F. Bear, and R. L. Huganir. Regulation of distinct ampa receptor phosphorylation sites during bidirectional synaptic plasticity. *Nature*, 405(6789):955, 2000.

[36] S.-J. R. Lee, Y. Escobedo-Lozoya, E. M. Szatmari, and R. Yasuda. Activation of camkii in single dendritic spines during long-term potentiation. *Nature*, 458(7236):299, 2009.

[37] S. Linse, A. Helmersson, and S. Forsen. Calcium binding to calmodulin and its globular domains. *Journal of Biological Chemistry*, 266(13):8050–8054, 1991.

[38] J. Lisman, H. Schulman, and H. Cline. The molecular basis of camkii function in synaptic and behavioural memory. *Nature Reviews Neuroscience*, 3(3):175, 2002.

[39] J. Lisman, R. Yasuda, and S. Raghavachari. Mechanisms of camkii action in long-term potentiation. *Nature reviews neuroscience*, 13(3):169, 2012.

[40] S. R. MARTIN, J. F. MAUNE, K. BECKINGHAM, and P. M. BAYLEY. Stopped-flow studies of calcium dissociation from calcium-binding-site mutants of drosophila melanogaster calmodulin. *European journal of biochemistry*, 205(3):1107–1117, 1992.

[41] T. Meyer, P. I. Hanson, L. Stryer, and H. Schulman. Calmodulin trapping by calcium-calmodulin-dependent protein kinase. *Science*, 256(5060):1199–1202, 1992.

[42] S. G. Miller and M. B. Kennedy. Regulation of brain type ii ca2+ calmodulin-dependent protein kinase by autophosphorylation: A ca2+-triggered molecular switch. *Cell*, 44(6):861–870, 1986.

[43] S. G. Miller, B. L. Patton, and M. B. Kennedy. Sequences of autophosphorylation sites in neuronal type ii cam kinase that control ca2+-independent activity. *Neuron*, 1(7):593–604, 1988.

[44] V. N. Murthy, T. Schikorski, C. F. Stevens, and Y. Zhu. Inactivity produces increases in neurotransmitter release and synapse size. *Neuron*, 32(4):673–682, 2001.

[45] J. B. Myers, V. Zaegel, S. J. Coultrap, A. P. Miller, K. U. Bayer, and S. L. Reichow. The camkii holoenzyme structure in activation-competent conformations. *Nature communications*, 8:15742, 2017.

[46] E. Neher and G. Augustine. Calcium gradients and buffers in bovine chromaffin cells. *The Journal of physiology*, 450(1):273–301, 1992.

[47] T. Nevian and B. Sakmann. Spine ca2+ signaling in spike-timing-dependent plasticity. *Journal of Neuroscience*, 26(43):11001–11013, 2006.

[48] E. A. Nimchinsky, R. Yasuda, T. G. Oertner, and K. Svoboda. The number of glutamate receptors opened by synaptic stimulation in single hippocampal spines. *Journal of Neuroscience*, 24(8):2054–2064, 2004.

[49] K.-I. Okamoto, R. Narayanan, S. H. Lee, K. Murata, and Y. Hayashi. The role of camkii as an f-actin-bundling protein crucial for maintenance of dendritic spine structure. *Proceedings of the National Academy of Sciences*, 104(15):6418–6423, 2007.

[50] P. Opazo and D. Choquet. A three-step model for the synaptic recruitment of ampa receptors. *Molecular and Cellular Neuroscience*, 46(1):1–8, 2011.

[51] B. L. Patton, S. G. Miller, and M. B. Kennedy. Activation of type ii calcium/calmodulin-dependent protein kinase by ca2+/calmodulin is inhibited by autophosphorylation of threonine within the calmodulin-binding domain. *Journal of Biological Chemistry*, 265(19):11204–11212, 1990.

[52] O. B. Peersen, T. S. Madsen, and J. J. Falke. Intermolecular tuning of calmodulin by target peptides and proteins: differential effects on ca2+ binding and implications for kinase activation. *Protein Science*, 6(4):794–807, 1997.

[53] S. Pepke, T. Kinzer-Ursem, S. Mihalas, and M. B. Kennedy. A dynamic model of interactions of ca2+, calmodulin, and catalytic subunits of ca2+/calmodulin-dependent protein kinase ii. *PLoS computational biology*, 6(2):e1000675, 2010.

[54] A. Persechini, H. D. White, and K. J. Gansz. Different mechanisms for ca dissociation from complexes of calmodulin with nitric oxide synthase or myosin light chain kinase. *Journal of Biological Chemistry*, 271(1):62–67, 1996.

[55] J. J. Petrozzino, L. D. P. Miller, and J. A. Connor. Micromolar ca2+ transients in dendritic spines of hippocampal pyramidal neurons in brain slice. *Neuron*, 14(6):1223–1231, 1995.

[56] P. Rangamani, M. G. Levy, S. Khan, and G. Oster. Paradoxical signaling regulates structural plasticity in dendritic spines. *Proceedings of the National Academy of Sciences*, 113(36):E5298–E5307, 2016.

[57] R. C. Rich and H. Schulman. Substrate-directed function of calmodulin in autophosphorylation of ca2+/calmodulin-dependent protein kinase ii. *Journal of Biological Chemistry*, 273(43):28424–28429, 1998.

[58] O. S. Rosenberg, S. Deindl, R.-J. Sung, A. C. Nairn, and J. Kuriyan. Structure of the autoinhibited kinase domain of camkii and saxs analysis of the holoenzyme. *Cell*, 123(5):849–860, 2005.

[59] B. L. Sabatini, T. G. Oertner, and K. Svoboda. The life cycle of ca2+ ions in dendritic spines. *Neuron*, 33(3):439–452, 2002.

[60] K. Shen, M. N. Teruel, K. Subramanian, and T. Meyer. Camkiiβ functions as an f-actin targeting module that localizes camkiiα/β heterooligomers to dendritic spines. *Neuron*, 21(3):593–606, 1998.

[61] J. M. Shifman, M. H. Choi, S. Mihalas, S. L. Mayo, and M. B. Kennedy. Ca2+/calmodulin-dependent protein kinase ii (camkii) is activated by calmodulin with two bound calciums. *Proceedings of the National Academy of Sciences*, 103(38):13968–13973, 2006.

[62] A. J. Silva, R. Paylor, J. M. Wehner, and S. Tonegawa. Impaired spatial learning in alpha-calcium-calmodulin kinase ii mutant mice. *Science*, 257(5067):206–211, 1992.

[63] A. J. Silva, C. F. Stevens, S. Tonegawa, and Y. Wang. Deficient hippocampal long-term potentiation in alpha-calcium-calmodulin kinase ii mutant mice. *Science*, 257(5067):201–206, 1992.

[64] M. W. Sneddon, J. R. Faeder, and T. Emonet. Efficient modeling, simulation and coarse-graining of biological complexity with nfsim. *Nature methods*, 8(2):177, 2011.

[65] S. Strack, S. Choi, D. M. Lovinger, and R. J. Colbran. Translocation of autophosphorylated calcium/calmodulin-dependent protein kinase ii to the postsynaptic density. *Journal of Biological Chemistry*, 272(21):13467–13470, 1997.

[66] K. Takao, K.-I. Okamoto, T. Nakagawa, R. L. Neve, T. Nagai, A. Miyawaki, T. Hashikawa, S. Kobayashi, and Y. Hayashi. Visualization of synaptic ca2+/calmodulin-dependent protein kinase ii activity in living neurons. *Journal of Neuroscience*, 25(12):3107–3112, 2005.

[67] J.-J. Tapia, A. S. Saglam, J. Czech, R. Kuczewski, T. M. Bartol, T. J. Sejnowski, and J. R. Faeder. Mcell-r: A particle-resolution network-free spatial modeling framework. In *Modeling Biomolecular Site Dynamics*, pages 203–229. Springer, 2019.

[68] K. F. Tolias, J. B. Bikoff, A. Burette, S. Paradis, D. Harrar, S. Tavazoie, R. J. Weinberg, and M. E. Greenberg. The rac1-gef tiam1 couples the nmda receptor to the activity-dependent development of dendritic arbors and spines. *Neuron*, 45(4):525–538, 2005.

[69] G.-Y. Wu and H. T. Cline. Stabilization of dendritic arbor structure in vivo by camkii. *Science*, 279(5348):222–226, 1998.

[70] Z. Xia and D. R. Storm. The role of calmodulin as a signal integrator for synaptic plasticity. *Nature Reviews Neuroscience*, 6(4):267, 2005.

[71] Z. Xie, D. P. Srivastava, H. Photowala, L. Kai, M. E. Cahill, K. M. Woolfrey, C. Y. Shum, D. J. Surmeier, and P. Penzes. Kalirin-7 controls activity-dependent structural and functional plasticity of dendritic spines. *Neuron*, 56(4):640–656, 2007.

[72] S.-N. Yang, Y.-G. Tang, and R. S. Zucker. Selective induction of ltp and ltd by postsynaptic [ca2+] i elevation. *Journal of neurophysiology*, 81(2):781–787, 1999.

[73] A. M. Zhabotinsky, R. N. Camp, I. R. Epstein, and J. E. Lisman. Role of the neurogranin concentrated in spines in the induction of long-term potentiation. *Journal of Neuroscience*, 26(28):7337–7347, 2006.

[74] J. J. Zhu, Y. Qin, M. Zhao, L. Van Aelst, and R. Malinow. Ras and rap control ampa receptor trafficking during synaptic plasticity. *Cell*, 110(4):443–455, 2002.

[75] D.-J. Zou and H. T. Cline. Postsynaptic calcium/calmodulin-dependent protein kinase ii is required to limit elaboration of presynaptic and postsynaptic neuronal arbors. *Journal of Neuroscience*, 19(20):8909–8918, 1999.